Proceedings of the
International Conference on Mechanical Engineering 2009
(ICME2009) 26- 28 December 2009, Dhaka, Bangladesh

ICME09-FM-14

ENTRANCE FLOW THROUGH ROTATING CURVED PIPE OF CIRCULAR CROSS-SECTION

M. A. Masud and M. Mahmud Alam

Mathematics Discipline, Khulna University, Khulna, Bangladesh

ABSTRACT

A numerical study is performed regarding entrance flow of a viscous incompressible fluid through rotating curved pipe of circular cross-section. The flow depends on the pressure gradient force, centrifugal force due to curvature and coriolis force due to rotation. The effects of all these forces result in interesting flow behaviours in the entry region which are analyzed in the present study. The mathematical model is established considering three dimensional momentum equation. The problem is solved by finite difference method in a computational mesh extending from the inlet immediately adjacent to the reservoir to the fully developed region.

Keywords: Entry Flow, Rotation, Curved Pipe.

1. INTRODUCTION

Fluid flow in curved pipes is of considerable importance. It has large applications in chemical and mechanical engineering. Curved tube geometries are also found in bio-fluid-mechanics. It is extensively used in piping systems such as intakes in aircraft.

In case of curved pipe centrifugal force originates due to the curvature of the pipe. For flow through a straight pipe, the axial velocity in the core region is much master than that near the wall which is due to no-slip condition at the wall. But when the fluid flows through a curved pipe, the particles experience centrifugal force which brings about the secondary flow. This was first noticed by Williams et al.[1]. They also found that the location of the maximum axial velocity is shifted towards the outer wall as an effect of the occurrence of secondary flow.

Dean [2,3] was the foremost author to formulate the problem theoretically. Here incompressible viscous fluid flow under constant pressure gradient force has been investigated and the flow is found to be dependent on a parameter termed as Dean number D_n given by $D_n = \frac{a^3}{\mu\upsilon}\sqrt{\frac{2a}{L}}G$; where, μ is the coefficient of viscosity, υ is the kinematic viscosity, G is the constant pressure gradient force, L is the radius of the pipe and a is the radius of the cross-section.

After this, a lot of research works regarding fully developed flow have been carried out at different times. But in practice the flow is not always fully developed. So developing or entry flow is of utmost importance specially incase of physiological phenomena. Austin [4], Patankar et al. [5] and Humphery [6] carried out study on developing flow through curved pipe beginning with Poiseuille flow at the inlet using finite-difference technique. Singh [7] obtained a series solution for the entry-flow problem. He found a saddle-point-like stagnation point and a node-like sink near and at the centre of the pipe. Yao and Berger [8] obtained a solution for the flow from the entry to the fully developed region. Soh and Berger [9] solved elliptic Navier-Stokes equation for entrance flow into a curved pipe using the artificial compressibility technique. Secondary flow separation was observed near the inner wall in the developing region of the curved pipe.

But if the curved pipe rotates, in addition to centrifugal force the fluid experience Coriolis force. The rotation is considered to be positive if it is in such a direction that the Coriolis force results a positive effect to that of the centrifugal force and this case is known as co-rotating case. Otherwise the rotation is considered to be negative and is known as counter rotating case. These types of rotating ducts are used in cooling systems for conductors of electric generators.

Since the pipelines have more or less a bent or a curved section, it is interesting to investigate the combined effects of curvature and rotation, which are relevant to the flow in rotating curved ducts. Miyazaki [10] examined the solutions for co-rotating case. Ito and Motai [11] investigated both co-rotating and counter rotating cases. At this time the concept of bifurcation was not so rich. Later Daskopoulos and Lenhoff [12] showed the bifurcation study of the flow combined with curvature and rotation.

In this paper, our aim is to study the entrance flow through a curved pipe of circular cross-section rotating at a constant angular velocity about an axis passing through the center of curvature of the pipe and perpendicular to the plane of the pipe.

2. GOVERNING EQUATIONS

A curved pipe of uniform circular cross-section has been considered. The pipe is rotating at a constant angular velocity about an axis passing through the centre of curvature of the pipe and perpendicular to the plane containing the axis of the pipe. The radius of the pipe is R and the radius of the cross-section is a. Toroidal coordinate system (r', θ, s') has been considered to describe the motion of the fluid particles in the pipe which is illustrated in Fig 1. u', v', w' are the velocity components along r', θ, s' directions respectively, p' is the pressure and ρ is the constant density of the fluid.

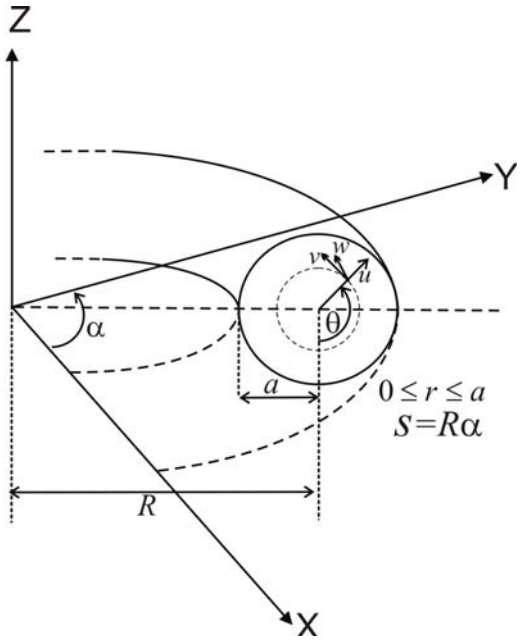

Fig 1. Toroidal coordinate system for a curved pipe with circular cross-section.

Introducing the non-dimensional variables,

$$u = \frac{u'}{W_\circ}, v = \frac{v'}{W_\circ}, w = \frac{w'}{W_\circ}, p = \frac{p'}{\rho W_\circ^{\,2}}, r = \frac{r'}{a}$$

we get the following momentum equations,

radial momentum equation,

$$\frac{1}{r\omega}\left[\frac{\partial}{\partial s}(ruw)+\frac{\partial}{\partial r}\left(r\omega u^2\right)+\frac{\partial}{\partial\theta}(\omega uv)-\omega v^2-\delta r w^2\sin\theta\right]-T_r v$$
$$=-\frac{\partial p_1}{\partial r}+\frac{1}{R_e}\left[\frac{1}{r\omega}\left\{\frac{\partial}{\partial r}\left(r\omega\frac{\partial u}{\partial r}\right)+\frac{\partial}{\partial\theta}\left(\frac{\omega}{r}\frac{\partial u}{\partial\theta}\right)+\frac{\partial}{\partial s}\left(\frac{r}{\omega}\frac{\partial u}{\partial s}\right)\right\}\right.$$
$$\left.-\frac{1}{r^2}\left(2\frac{\partial v}{\partial\theta}+u\right)-\frac{v\delta}{\omega r}\cos\theta-\frac{\delta^2}{\omega^2}\left(\frac{2}{\delta}\frac{\partial w}{\partial s}+u\sin\theta+v\cos\theta\right)\sin\theta\right. \quad (1)$$

circumferential momentum equation,

$$\frac{1}{r\omega}\left[\frac{\partial}{\partial s}(rvw)+\frac{\partial}{\partial r}(ruv\omega)+\frac{\partial}{\partial\theta}\left(\omega v^2\right)+\omega uv-\delta r w^2\cos\theta\right]-T_r u$$
$$=-\frac{1}{r}\frac{\partial p_1}{\partial\theta}+\frac{1}{R_e}\left[\frac{1}{r\omega}\left\{\frac{\partial}{\partial r}\left(r\omega\frac{\partial v}{\partial r}\right)+\frac{\partial}{\partial\theta}\left(\frac{\omega}{r}\frac{\partial v}{\partial\theta}\right)+\frac{\partial}{\partial s}\left(\frac{r}{\omega}\frac{\partial v}{\partial s}\right)\right\}\right.$$
$$\left.+\frac{1}{r^2}\left(2\frac{\partial u}{\partial\theta}-v\right)+\frac{u\delta}{\omega r}\cos\theta-\frac{\delta^2}{\omega^2}\left(\frac{2}{\delta}\frac{\partial w}{\partial s}+u\sin\theta+v\cos\theta\right)\cos\theta\right. \quad (2)$$

Axial momentum equation,

$$\frac{1}{r\omega}\left[\frac{\partial}{\partial s}\left(rw^2\right)+\frac{\partial}{\partial r}(r\omega uw)+\frac{\partial}{\partial\theta}(\omega vw)+rw\delta(u\sin\theta+v\cos\theta)\right]$$
$$=-\frac{1}{\omega}\frac{\partial p_1}{\partial s}+\frac{1}{R_e}\left[\frac{1}{r\omega}\left\{\frac{\partial}{\partial r}\left(r\omega\frac{\partial w}{\partial r}\right)+\frac{\partial}{\partial\theta}\left(\frac{\omega}{r}\frac{\partial w}{\partial\theta}\right)+\frac{\partial}{\partial s}\left(\frac{r}{\omega}\frac{\partial w}{\partial s}\right)\right\}\right.$$
$$\left.+\frac{2\delta^2}{\omega^2}\left(\frac{\sin\theta}{\delta}\frac{\partial u}{\partial s}-\frac{\cos\theta}{\delta}\frac{\partial v}{\partial s}-\frac{w}{2}\right)\right. \quad (3)$$

and the continuity equation takes the form,

$$\frac{\partial}{\partial r}(r\omega u)+\frac{\partial}{\partial\theta}(\omega v)+\frac{\partial}{\partial s}(rw)=0 \quad (4)$$

where, $R_e=\frac{aW_\circ}{\upsilon}$, $T_r=\frac{2a\Omega}{W_\circ}$, $\omega=1+r\delta\sin\theta$ and $\delta=\frac{a}{R}$.

3. BOUNDARY CONDITIONS

In the present study the fluid flow boundary is considered to be consists of three regions: the inlet cross-section where the fluid is entering, the rigid wall surrounding the fluid and the cross-section far downstream where the flow is assumed to be fully developed.

The initial conditions at the inlet is considered as,

$w(r,\theta,0)=\frac{1}{1+\delta r\sin\theta}$, $u(r,\theta,0)=v(r,\theta,0)=0$ and $p=-\frac{1}{2(1+\delta r\sin\theta)^2}$

Due to the no-slip condition, all the velocity components vanish at the rigid boundary, i.e.,

$$u(1,\theta,s)=v(1,\theta,s)=w(1,\theta,s)=0$$

At far down stream when the flow gets fully developed, $\frac{\partial u}{\partial s}=\frac{\partial v}{\partial s}=\frac{\partial w}{\partial s}=0$

4. FINITE DIFFERENCE FORMULATIONS

To rewrite the momentum equations (1-3) and 4 into a practical finite-difference scheme of computation , the grid arrangement shown in Fig 2 and Fig 3 has been chosen. The grid has been arranged in such a way that pressure is defined at the centre of a cell and u, v, w are defined at different positions on the pressure cell boundaries.

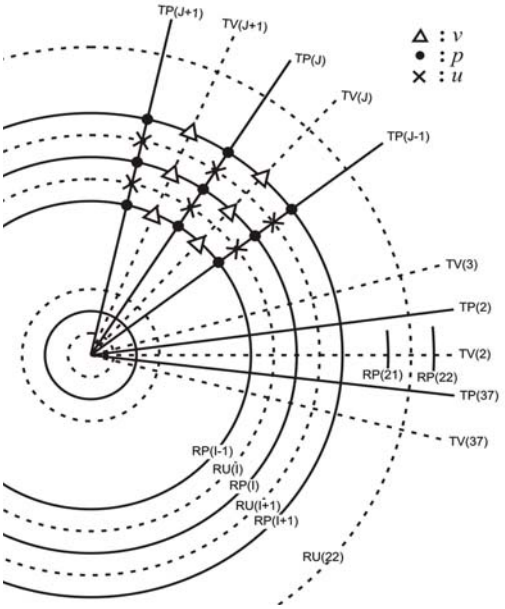

Fig 2. Grid system in the cross-section.

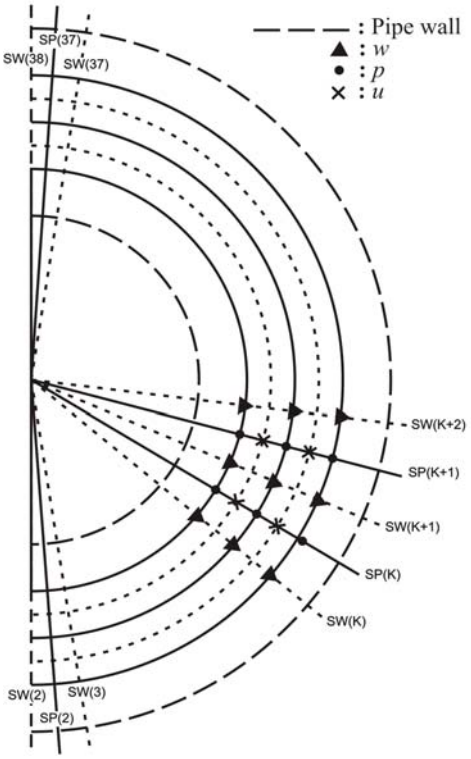

Fig 3. Grid system in the horizontal plane passing through the axis of the pipe.

Then the momentum equations in u, v, w-directions reduces to,

$$a^u_{ijk}u_{ijk} = a^u_{i+1\,jk}u_{i+1\,jk} + a^u_{i-1\,jk}u_{i-1\,jk} + a^u_{ij+1k}u_{ij+1k} + a^u_{ij-1k}u_{ij-1k} + a^u_{ijk+1}u_{ijk+1} + a^u_{ijk-1}u_{ijk-1} + b^u + A^u_{ijk}\left(p_{i-1\,jk} - p_{ijk}\right)$$

$$a^v_{ijk}v_{ijk} = a^v_{i+1\,jk}v_{i+1\,jk} + a^v_{i-1\,jk}v_{i-1\,jk} + a^v_{ij+1k}v_{ij+1k} + a^v_{ij-1k}v_{ij-1k} + a^v_{ijk+1}v_{ijk+1} + a^v_{ijk-1}v_{ijk-1} + b^v + A^v_{ijk}\left(p_{ij-1k} - p_{ijk}\right)$$

$$a^w_{ijk}w_{ijk} = a^w_{i+1\,jk}w_{i+1\,jk} + a^w_{i-1\,jk}w_{i-1\,jk} + a^w_{ij+1k}w_{ij+1k} + a^w_{ij-1k}w_{ij-1k} + a^w_{ijk+1}w_{ijk+1} + a^w_{ijk-1}w_{ijk-1} + b^w + A^w_{ijk}\left(p_{ijk-1} - p_{ijk}\right)$$

respectively. And the continuity equation reduces to,

$$a_p p'_p = a_E p'_E + a_W p'_W + a_N p'_N + a_S p'_S + a_T p'_T + a_B p'_B + b$$

The accuracy is assured by taking $DIF < 10^{-6}$, where

$$DIF = \sum\sum\sum \begin{matrix} \{u_{n+1}(i,j,k) - u_n(i,j,k)\}^2 + \\ \{v_{n+1}(i,j,k) - v_n(i,j,k)\}^2 + \\ \{w_{n+1}(i,j,k) - w_n(i,j,k)\}^2 \end{matrix}$$

5. RESULTS AND DISCUSSION

Calculations were carried out for $\mathrm{Re} = 242 \,\&\, 900$ and $\delta = 0.1$ in a computational mesh extending from inlet(0°) to the outlet(180°).

5.1 Secondary Flow Development

Vector plots of the secondary flow have been shown in Fig 4(a) and 4(b) for $\mathrm{Re} = 242 \,\&\, 900$ respectively at different positions. The secondary flow is set up just after entering the inlet due to the effect of centrifugal force. Most of the particles get radial velocity. Circumferential velocity is greater for the particles near the upper and lower boundary due to the friction with the wall. Also the velocity of the particles at the centre of cross-section is radially outward for the effect of centrifugal force. As the flow goes downstream the secondary velocity of the particles near the centre of the cross-section increase in the direction of the centrifugal force and the flow in the core region moves radially outward along the horizontal plane passing through the centre of the cross-section. At the same time, the particles near the upper and lower boundary experience high circumferential velocity in the direction opposite to the velocity of the particles at the core region. As a result, two vortex secondary flow is set up, which is symmetric about the horizontal plane passing through the centre of cross-section.

Increase in Reynold's number decrease the velocity of he particles near the core region remarkably. For $\mathrm{Re} = 900$ the secondary velocity of the particles in the inner half is higher than the velocity of the particles at the centre and outer half of the cross-section. As a result, two vortices are set up in the inner half. The strength of these vortices is lower than that of the vortices for $\mathrm{Re} = 242$.

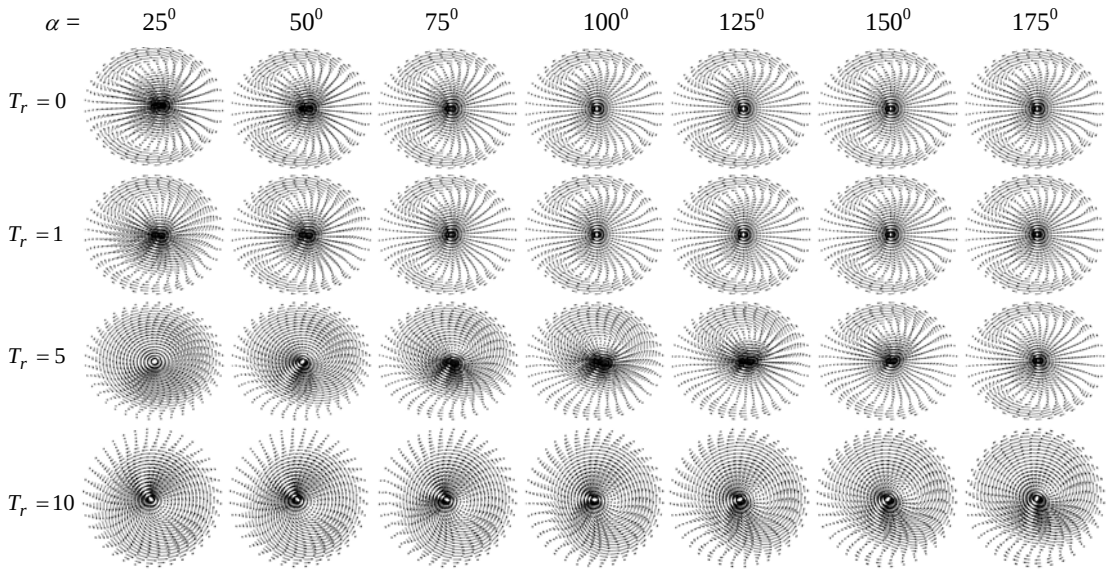

Fig 4a. Vector plots of the secondary flow for $R_e = 242$ and $\delta = 0.1$

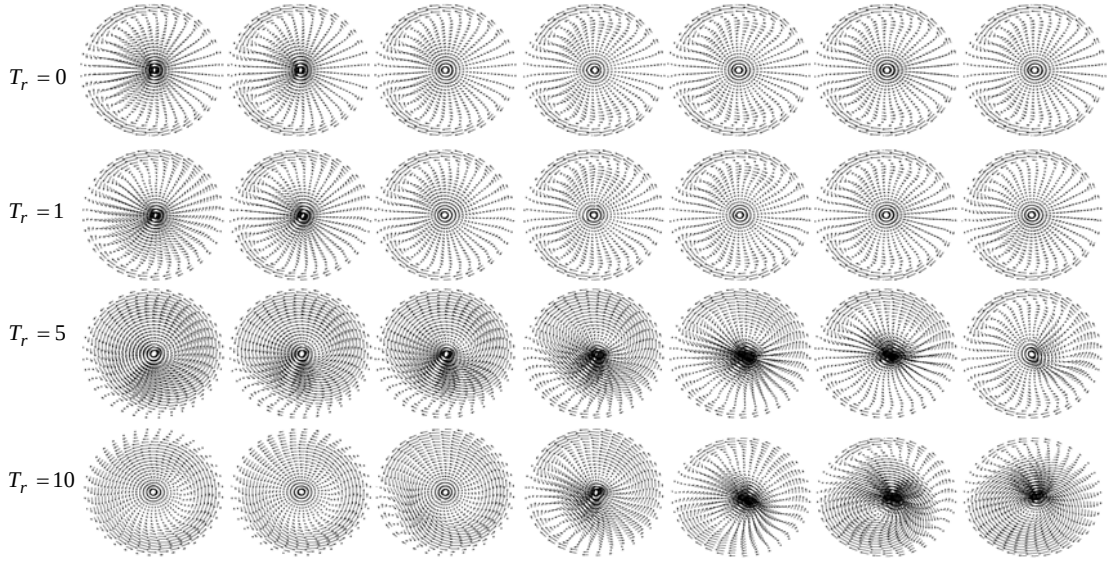

Fig 4b. Vector plots of the secondary flow for $R_e = 900$ and $\delta = 0.1$

When rotation comes to play, centrifugal force and Coriolis force work simultaneously in addition to pressure gradient force. The Coriolis force breaks down the symmetry. The particles get high circumferential velocity due to Coriolis force. As the flow proceed downstream a vortex originates form the lower portion and two vortex secondary flow is set up. Gradually the lower vortex gets stronger. At far downstream the centrifugal force prevails over Coriolis force and the secondary flow become symmetric. If rotation is increased the Coriolis force increases and consequently the flow needs to traverse more towards downstream to be symmetric. For high rotation $(T_r = 10)$ remain asymmetric even at the outlet.

5.2 Axial Flow Development

The contour plots of the axial velocity has been shown in Fig 5(a) and 5(b) for $\mathrm{Re} = 242 \,\&\, 900$ respectively. As the flow enters the pipe boundary layer begins to develop. Boundary layer near the inner wall develops faster than that at the outer wall. And with the development of the flow the strength of the axial flow is increased and is shifted towards the outer wall of the cross-section, which is effect of the centrifugal force due to curvature. The axial flow is symmetric about the plane passing through the centre of cross-section at the absence of rotation.

When the pipe rotates the symmetry breaks down. Due to Coriolis force the strength of the axial flow is shifted towards the lower portion of the cross-section. As the flow proceeds downstream the strength of the axial flow is shifted towards the middle of the outer half. Finally the centrifugal force dominates the Coriolis force and symmetry is attained. But for higher rotation the Coriolis force is too high to be dominated by the centrifugal force. As a result symmetry is not attained finally.

For high rotation initially two peaked axial velocity is found. With the development of the flow the outer peak diminishes while the inner peak develops and gradually shifted outward. Finally, it took place diagonally between the upper part of the outer half and lower part of the inner half.

For $\mathrm{Re} = 900$ symmetric axial velocity profile has been found which is strong in the outer half when rotation is absent. When $T_r = 10$ two peaked axial velocity is found, one peak in the inner half and another in the outer half. With the development of the flow the vortices took place in the upper and lower half of the cross-section respectively.

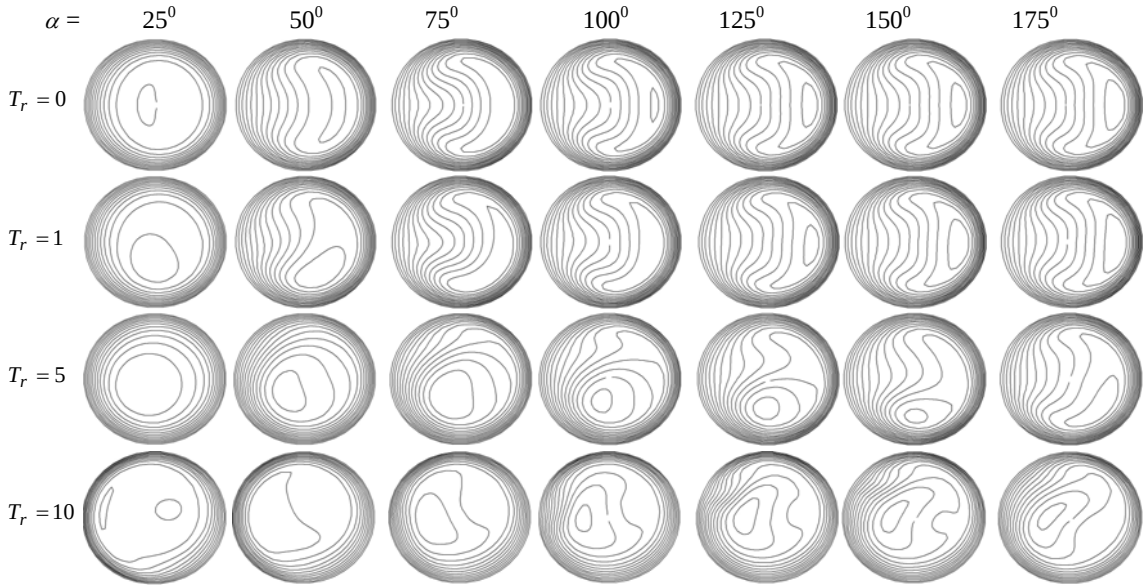

Fig 5a. Contour plots of the axial flow for $R_e = 242$ and $\delta = 0.1$

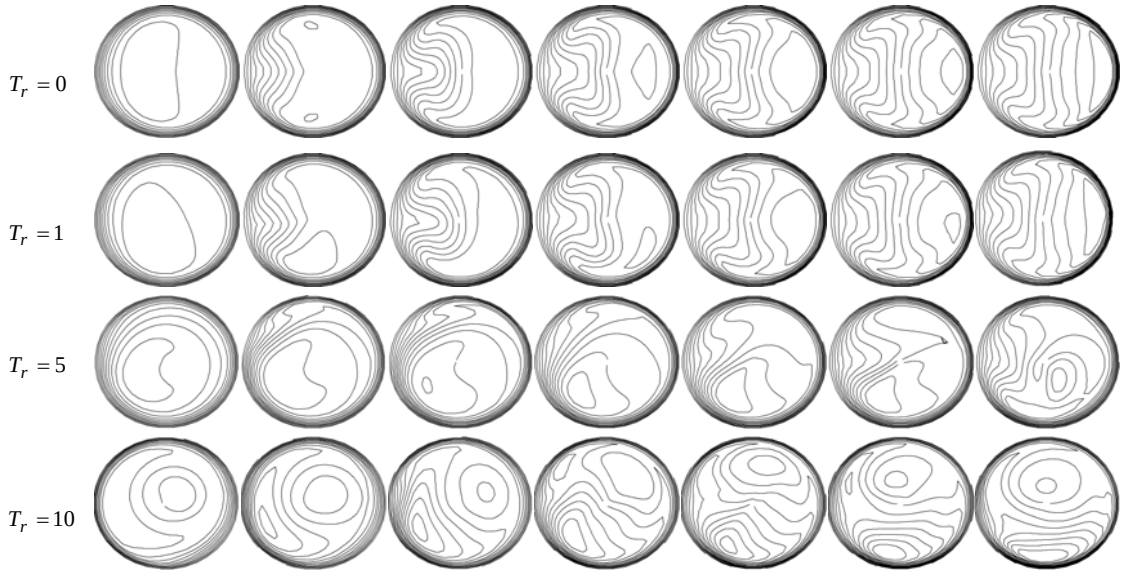

Fig 5b. Contour plots of the axial flow for $R_e = 900$ and $\delta = 0.1$

6. REFERENCES

1. Williams, G. S., Hubbell, C. W. and Finkell, G. H., 1902, "Experiments at Detroit, Michigan on the effect of curvature on the flow of water in pipes", Trans. ASCE, 47:1-196.
2. Dean, W. R., 1927, "Note on the Motion of Fluid in a Curved Pipe", Philosophical Magazine and Journal of Science, 4(20):208-223.
3. Dean, W. R., 1928, "The Stream-line Motion of Fluid in a Curved Pipe", Philosophical Magazine and Journal of Science, 5(30):673-695.
4. Austin, L., 1971, *The development of viscous flow within helical coils*, Ph. D. thesis, University of Utah, Salt Lake City.
5. Patankar., S. V., Pratap, V. S. and Spalding, D. B., 1974, "Prediction of laminar flow and heat transfer in helically coiled pipes", Journal of Fluid Mechanics, 62:539.
6. Humphery, J. A. C., 1977, *Flow in ducts with curvature and roughness*. Ph. D. thesis, Imperial College of Science and Technology.
7. Singh, M. P., 1974, "Entry flow in a curved pipe", Journal of Fluid Mechanics, 65:517.
8. Yao, L. S. and Berger, S. A., 1975, "Entry flow in a curved pipe", Journal of Fluid Mechanics, 88: 339.
9. Soh, W. Y. and Berger, S. A., 1984, "Laminar entrance flow in a curved pipe", Journal of Fluid Mechanics, 148:109-135.
10. Miyazaki, H., 1971, "Combined free- and forced-convective heat transfer and fluid flow in rotating curved circular tube", International Journal of heat mass transfer, 14:1295-1309.
11. Ito, H. and Motai T., 1974, "Secondary flow in rotating curved pipe", The reports of the Institute of high speed Mechanics, Tohoku University, Sendai, Japan, 29(270):33-57.
12. Daskopoulos, P. and Lenhoff, A. M., 1990, "Flow in curved ducts: Part 2. Rotating ducts", Journal of Fluid Mechanics, 217:575-593.

7. NOMENCLATURE

Symbol	Meaning
u,v,w	Dimensionless velocity components along radial, circumferential and axial direction respectively
R_e	Reynold's Number
T_r	Taylor Number
δ	Dimensionless curvature

8. MAILING ADDRESS

Md. Mahmud Alam
Mathematics Discipline,
Khulna University, Khulna-9208, Bangladesh
E-mail: alam_mahmud2000@yahoo.com